ARCHIVAL REPORT

In Vivo Ketamine-Induced Changes in [^{11}C]ABP688 Binding to Metabotropic Glutamate Receptor Subtype 5

Christine DeLorenzo, Nicole DellaGioia, Michael Bloch, Gerard Sanacora, Nabeel Nabulsi, Chadi Abdallah, Jie Yang, Ruofeng Wen, J. John Mann, John H. Krystal, Ramin V. Parsey, Richard E. Carson, and Irina Esterlis

Background: At subanesthetic doses, ketamine, an *N*-methyl-D-aspartate glutamate receptor antagonist, increases glutamate release. We imaged the acute effect of ketamine on brain metabotropic glutamatergic receptor subtype 5 with a high-affinity positron emission tomography (PET) ligand [^{11}C]ABP688 (*E*)-3-[2-(6-methyl-2-pyridinyl)ethynyl]-2-cyclohexen-1-one-*O*-(methyl-$_{11}$C)oxime, a negative allosteric modulator of the metabotropic glutamatergic receptor subtype 5.

Methods: Two [^{11}C]ABP688 PET scans were performed in 10 healthy nonsmoking human volunteers (34 ± 13 years old); the two PET scans were performed on the same day—before (scan 1) and during intravenous ketamine administration (.23 mg/kg over 1 min, then .58 mg/kg over 1 hour; scan 2). The PET data were acquired for 90 min immediately after [^{11}C]ABP688 bolus injection. Input functions were obtained through arterial blood sampling with metabolite analysis.

Results: A significant reduction in [^{11}C]ABP688 volume of distribution was observed in scan 2 relative to scan 1 of 21.3% ± 21.4%, on average, in the anterior cingulate, medial prefrontal cortex, orbital prefrontal cortex, ventral striatum, parietal lobe, dorsal putamen, dorsal caudate, amygdala, and hippocampus. There was a significant increase in measurements of dissociative state after ketamine initiation ($p < .05$), which resolved after completion of the scan.

Conclusions: This study provides first evidence that ketamine administration decreases [^{11}C]ABP688 binding in vivo in human subjects. The results suggest that [^{11}C]ABP688 binding is sensitive to ketamine-induced effects, although the high individual variation in ketamine response requires further examination.

Key Words: Brain, [^{11}C]ABP688, glutamate, ketamine, mGluR5, PET

Glutamate, the principal excitatory neurotransmitter, is found throughout the brain, and alterations in the glutamatergic system have been implicated in various disorders, including addiction (1–3), major depressive disorder (4–6), and bipolar disorder (7). Glutamate may contribute to abnormalities in sleep, appetite, motivation, and concentration (8). Altering the glutamatergic system may lead to improvements in functioning, and glutamatergic agents are being actively evaluated as potential rapidly acting antidepressants (9–12).

Ketamine, a noncompetitive *N*-methyl-D-aspartate glutamate receptor antagonist, has been studied extensively for its capacity to produce a rapid antidepressant response (within 4–24 hours) in patients with treatment-resistant depression (11,13–16). The neurobiology underlying the antidepressant effects of ketamine is being explicated by current research. Perhaps as a consequence of its ability to reduce the recruitment of γ-aminobutyric acid interneurons, administration of subanesthetic ketamine doses stimulates or disinhibits cortical glutamate release, as measured in rodents with in vivo microdialysis (17,18) and carbon-13 magnetic resonance spectroscopy (19) and in humans with hydrogen-1 magnetic resonance spectroscopy (20). Improving understanding of the cascade of events that occur after glutamate release is necessary to provide insight into the mechanism of action of ketamine. For example, glutamate release produced by ketamine stimulates alpha-amino-3-hydroxy-5-methyl-4-isoxazole propionic acid receptors, enhancing downstream signaling mechanisms, such as the mammalian target of rapamycin pathway (21). Enhanced signaling rapidly increases dendritic spine production, reversing deficits in spines associated with the unpredictable stress model in rats (22). The disinhibition in cortical networks produced by ketamine is reflected in increased resting state cortical functional connectivity, as measured with functional magnetic resonance imaging (MRI) (23,24). However, much is still unknown about the downstream effects at other glutamate receptors.

The purpose of the present study was to explore whether increases in glutamate release produced by ketamine administration in humans would be reflected in reductions in ligand binding to metabotropic glutamatergic receptor subtype 5 (mGluR5). Generally, there are parallels between the proposed approach and paradigms employed to characterize changes in neurotransmitters such as γ-aminobutyric acid, acetylcholine, and dopamine release in psychiatric illness and other diseases (25–29). In those cases, the radioligand and the neurotransmitter bind to

From the Departments of Psychiatry (CD, RVP), Biomedical Engineering (CD), Radiology (RVP), Preventive Medicine (JY), and Applied Mathematics and Statistics (RW), Stony Brook University, Stony Brook; Department of Psychiatry (CD, JJM), Columbia University, New York, New York; Departments of Psychiatry (ND, MB, GS, CA, JHK, IE), Diagnostic Radiology (NN, REC, IE), Biomedical Engineering (REC), and Child Study Center (MB), Yale University, New Haven; and Clinical Neuroscience Division (CA, JHK), National Center for PTSD, VA Connecticut Healthcare System, West Haven, Connecticut.

Address correspondence to Christine DeLorenzo, Ph.D., Department of Psychiatry, Stony Brook University, HSC-T10-040D, Stony Brook, NY 11794; E-mail: Christine.DeLorenzo@stonybrookmedicine.edu.

Received Mar 24, 2014; revised Jun 17, 2014; accepted Jun 23, 2014.

0006-3223/$36.00
http://dx.doi.org/10.1016/j.biopsych.2014.06.024

the same site. However, the available ligands for measurement of mGluR5 using positron emission tomography (PET) ([^{18}F]FPEB (30,31), [^{11}C]ABP688 (4,32–34), and [^{11}C]SP203 (35)) are negative allosteric modulators. In contrast to previous studies, the present study explores the hypothesis that glutamate released during the infusion of ketamine, a drug that does not bind to mGluR5 with high affinity, would reduce [^{11}C]ABP688 binding to mGluR5 through mechanisms other than direct competition.

Methods and Materials

Subjects

This study was approved by the Yale University Institutional Review Board and Radiation Safety Committee and by the Yale–New Haven Hospital Radiation Safety Committee. After completing the informed consent process, inclusion criteria were assessed by the following: physical examination, routine blood tests, and psychiatric and neurologic examination. A urine drug screen, electrocardiogram, and pregnancy test (for women) were performed at screening and before radiotracer administration. General inclusion criteria were as follows: 1) age 18–60 years old; 2) English speaking; 3) no current, or history of, any DSM-IV diagnosis; 4) no first-degree relative with history of psychotic, mood, or anxiety disorder; and 5) no recent regular medication use and no history of psychiatric medication use. There were 13 subjects deemed eligible to participate in the study. Of the 13 subjects, 1 subject was withdrawn from the study after the baseline PET scan because of high blood pressure (before ketamine administration), and 2 subjects could not tolerate the full ketamine dose and were unable to continue with the scanning procedures so their data were discarded. The study was completed by 10 healthy nonsmoking volunteers (5 men and 5 women; mean age, 33.5 ± 13.2 years).

Psychiatric Assessments

Psychiatric history and a Structured Clinical Interview for DSM, Non-patient Edition, were conducted at screening. The Hamilton Depression Rating Scale (36), Montgomery–Åsberg Depression Rating Scale (37), and Beck Depression Inventory (38) were used to assess subjects' depressive symptoms during intake and on the day of PET scan (before and 30 min and 24 hours after ketamine administration). The effects of ketamine on subjects' mental state were subjectively assessed using the Clinician Administered Dissociative State Scale (CADSS) (39) and Profile of Mood States (40).

PET

High specific activity [^{11}C]ABP688 (1073 ± 370 MBq/nmol at end of synthesis) was produced from the reaction of [^{11}C]methyl iodide with desmethyl-ABP688 using the loop method developed by Nabulsi and described by Sandiego *et al.* (41). The average radiochemical and chemical purities were 97% (n = 20). The average E/Z isomer ratio in the final PET drug product was 70:1 (by radio-analytical high performance liquid chromatography area percent, with E being the major isomer). The E-isomer has been shown to exhibit a higher dissociation constant in vivo (42). A high-resolution research tomograph (Siemens Molecular Imaging, Knoxville, Tennessee) was used for PET imaging. A 6-min transmission scan was acquired before injection. The PET ligand [^{11}C]ABP688 was administered as a bolus over 1 min, and emission data were collected for 90 min in list mode. (We collected 90 min of data in case 60 min was insufficient to capture ketamine-induced effects; however, owing to the rapid effects of ketamine, this was not the case.) List-mode data collected over 60 min were used, binned into 14 frames (6 at 30 sec, 3 at 1 min, 2 at 2 min, and 10 at 5 min duration), based on previous analysis with this tracer that indicated that 60 min is sufficient (43,44). Head motion was recorded during the scan using a commercial optical tracking system, the Polaris Vicra system (Northern Digital Inc., Waterloo, Ontario, Canada). Images were reconstructed and corrected for attenuation, scatter, and motion using the motion-compensation ordered subset expectation maximization list-mode algorithm for resolution-recovery reconstruction (MOLAR) (45).

Following the baseline [^{11}C]ABP688 scan, subjects were given a short (~1 hour) break and then received the ketamine challenge scan. A second [^{11}C]ABP688 dose was administered over 1 min, and then ketamine was administered immediately after successful radioligand administration. This design was used to decrease subject burden in case of equipment failure and to ensure capture of the immediate effects of ketamine, given that it induces a rapid glutamate release. Vital signs (pulse, blood pressure, and oxygen saturation) were obtained before and after ketamine administration and during the ketamine infusion (at 5- to 10-min intervals).

Racemic ketamine was obtained from the Yale–New Haven Hospital Pharmacy and administered intravenously, as previously described (46,47) (initial bolus of .23 mg/kg over 1 min followed by constant infusion of .58 mg/kg per hour over 1 hour). This is a subanesthetic but psychotomimetic dose. This dosing regimen of ketamine was used, instead of the usual antidepressant dosing of .5 mg/kg over 40 min, to enhance statistical power by inducing a larger glutamate surge as suggested by prior ketamine studies (48–50). Both dosing regimens are similar in the fact that they result in comparable changes in cognition and perception but do not cause the anesthetic effect. At 5, 15, 30, and 75 min, blood ketamine levels were assessed, as previously described (47), in all subjects except for no. 10 (venous blood samples for ketamine analysis could not be drawn after study initiation). To perform delineation of anatomic regions on the PET data, images were coregistered with T1-weighted MRI acquired on a 3-T Trio imaging system (Siemens Medical Systems, Erlangen, Germany) with a voxel size of 1 × 1 × 1 mm.

Input Function Measurement

Before PET imaging, catheters were inserted in the radial artery and forearm veins for arterial blood sampling and radioisotope injection, respectively. Blood activity was measured continuously for the first 7 min after radiotracer administration and manually at 2, 4, 9, 12, 15, 20, 25, 30, 40, 50, and 60 min. Radioactivity was analyzed as described previously (51). After correction for delay and dispersion as previously described (52), the automated and manual plasma concentration values were merged and smoothed by convolution with a Gaussian function (full width at half-maximum = 24 sec).

A high-performance liquid chromatography assay of five of the arterial blood samples (at 0, 4, 12, 30, and 60 min) was used to establish unmetabolized parent compound levels (53). Unmetabolized parent fraction levels were fitted with a Hill function, which is described by three parameters (A, B, and C), in which percent parent compound = $A \times (t^B/[t^B + C]) + 1$, where t is time (54). The input function was calculated as the product of the interpolated parent fraction and the merged plasma counts. These combined data were then fitted as the combination of a straight line and the sum of three exponentials, describing the function before and after the peak, respectively, resulting in the metabolite-corrected arterial input function. Free fraction measurements were performed using an ultrafiltration technique (53). However, all measured free fraction values were 3% and considered unreliable, as has been shown previously (43).

Image Analysis

Image analysis was performed using MATLAB (MathWorks, Natick, Massachusetts). Subsequent frames of each PET study were registered to the eighth frame using the FMRIB Linear Image Registration Tool (FLIRT), version 5.0 (The Oxford Centre for Functional Magnetic Resonance Imaging of the Brain, Oxford, United Kingdom), to correct for residual subject motion that may not have been accounted for by the Polaris Vicra system. Probabilistic regions of interest were determined using nonlinear registration techniques as previously described (55). The mean PET image was then coregistered to the subject's MRI using a semiautomated technique (56). Time activity curves were generated from the mean of the measured activity, weighted by regional label probabilities, within a region over the time course of the PET acquisition.

Outcome Measure Calculation

Regional outcome measures were calculated using an unconstrained two-tissue compartment model, as previously validated for this tracer (44). For computational efficiency, the Logan graphical approach was used for voxel analysis (57). Given the unreliable free fraction values and lack of a reference region (58), volume of distribution (V_T; ratio of the concentration of the ligand in the region of interest to the concentration in the plasma at equilibrium) (59) was used as the outcome measure. Percent change in radioligand binding was calculated as $[(V_{T,baseline} - V_{T,ketamine})/V_{T,baseline}] \times 100$.

Statistical Analysis

To determine the significance of detected binding differences as a result of ketamine administration, a linear mixed-effects model with region as a fixed effect was applied to the data. The dependence structure among regions and scans from the same subject was modeled using the Kronecker product between unrestricted symmetry (to model the correlation among all regions) and compound symmetry (to model the correlation between two scans). The interaction term between region and scan was examined and removed from the model if appropriate. Linear mixed models for longitudinal data were also used to model change in patients' vital signs after ketamine administration. The dependence structure used in these models was compound symmetry. The paired comparisons of scores from subjective reports from two time points were carried out through Wilcoxon signed rank test. Both unadjusted p values and false discovery rate corrected values, based on the Benjamini and Hochberg method, were reported for these paired comparisons. All tests were two-sided, and all analyses were carried out using R 3.0.2 (R Foundation for Statistical Computing, Vienna, Austria; http://www.r-project.org/) and SAS 9.3 (SAS Institute Inc., Cary, North Carolina).

Results

Vital Signs and Subjective Report

On average, there was a significant increase in heart rate and blood pressure after start of ketamine compared with baseline (Table 1). After 30 min, both heart rate and blood pressure had mostly returned to baseline levels. Oxygen saturation levels remained relatively constant.

Significant changes in CADSS scores were observed. Baseline values (acquired before scan 1) were 0 for all subjects except subject no. 2, who reported a value of 1 for the CADSS 12 and derealization subscale. Subjects scored significantly higher on many CADSS subscales during the ketamine challenge compared with baseline (Figure 1). There were no significant differences between scores at baseline and study end (60 min after ketamine). There were no significant differences in the Profile of Mood States, Beck Depression Inventory, or Montgomery–Åsberg Depression Rating Scale scores during the ketamine challenge compared with baseline. The Hamilton Depression Rating Scale data were collected only at baseline for most subjects (Table 2).

Tracer Metabolism and Clearance

There were no significant differences between scans (scan 1, scan 2) in the injected dose (576 ± 136 MBq, 593 ± 116 MBq, $p = .63$), specific activity (215.2 ± 194.4 MBq/nmol, 246.4 ± 224.2 MBq/nmol, $p = .56$), or mass (1.1 ± .7 μg, 1.2 ± 1.0 μg, $p = .85$). To assess the potential effects of ketamine on tracer metabolism, the fitted average unmetabolized parent compound curves were evaluated before and after ketamine infusion. Two of the three parameters (A and B; see Input Function Measurement) used to fit the subjects' metabolite values were significantly different after ketamine versus before ketamine ($p = .02$ in both cases) indicating a potential ketamine-induced slowing of metabolism or tracer clearance. When the delivery rate of the [^{11}C]ABP688 from arterial plasma to the tissue was examined (K_1) (59), significant increases in this parameter were observed in a region-dependent manner ($p = .018$, linear mixed effects model). However, clearance values, calculated as the injected dose divided by the extrapolated area under the metabolite-corrected arterial input function (60), were not significantly different across scans (baseline, 99.3 ± 32.2 L/h; ketamine, 90.1 ± 27.7 L/h; $p = .23$).

Ketamine-Induced Change in [^{11}C]ABP688 Binding

A significant reduction in [^{11}C]ABP688 binding was observed qualitatively and quantitatively (Figures 2 and 3). After ketamine administration, [^{11}C]ABP688 binding (V_T) significantly decreased in a region-dependent manner compared with the baseline scan (all region-specific $p < .007$, linear mixed effects model, including

Table 1. Mean and Standard Deviation of Subjects' Vital Signs Before and During Ketamine Infusion Scan

Minutes After Ketamine	Systolic BP	Diastolic BP	Heart Rate	SPO_2 (%)
Baseline	125.9 ± 11.9	63.3 ± 8.4	65.6 ± 11.5	97.5 ± .7
4[a]	134.8 ± 23.0	87.2 ± 16.4[b]	73.3 ± 21.3[b]	97.9 ± .3
9[c]	147.3 ± 26.5[b]	70.6 ± 11.9[b]	78.3 ± 16.3[b]	97.4 ± 1.0
15[c]	139.7 ± 26.1[b]	70.2 ± 8.7[b]	77.3 ± 16.8[b]	97.8 ± .7[d]
20[e]	138.7 ± 15.4[b]	75.6 ± 16.9[b]	70.8 ± 11.5	97.5 ± 1.2[d]
25[c]	133.4 ± 17.2	69.9 ± 10.3[b]	75 ± 20.1[b]	97.5 ± .8[d]
30	134.8 ± 17.1	68.9 ± 8.8[b]	73.1 ± 14.5[b]	97 ± 1.1[d]
40[c]	130.8 ± 16.5	65.9 ± 7.2	65.1 ± 11.4	97.4 ± 1.2
50	131.4 ± 14.3	68 ± 8.3	66.2 ± 12.7	97.4 ± 1.0
60[c]	133.8 ± 14.2	68.9 ± 6.1[b]	65.8 ± 12.6	97.7 ± .7
75	134.9 ± 16	68.3 ± 7.5	68 ± 12.5	97.8 ± 1.1
90	133.8 ± 19.7	68.4 ± 9.8	70.4 ± 9.4	97.8 ± .9

BP, blood pressure; SPO_2, oxygen saturation.

[a]Third subject is missing all measurements at this time.

[b]Using two-tailed t tests based on a linear mixed model for longitudinal data, these values were significantly different from baseline at a false discovery rate of 10%.

[c]First subject is missing all measurements at this time.

[d]Seventh subject is missing Spo_2 measurements at these times.

[e]Ninth subject is missing all measurements at this time.

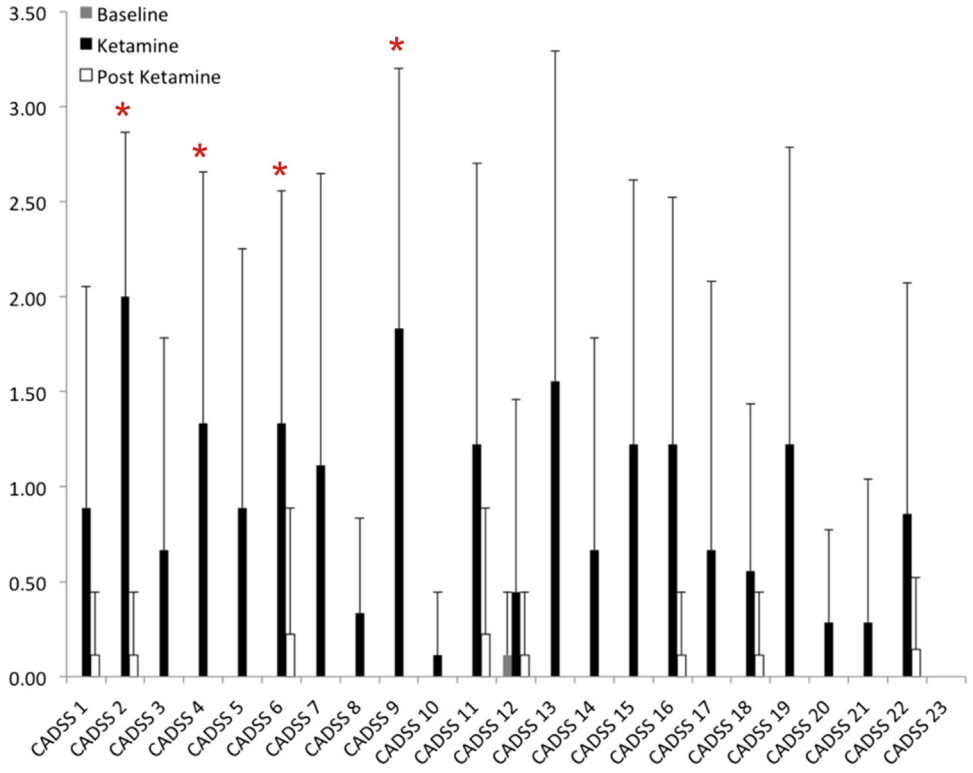

Figure 1. Average Clinician Administered Dissociative State Scale (CADSS) subscale scores at baseline (before scan 1) and during and after the ketamine challenge scan. These assessments were recorded for nine subjects ($n = 9$) except for CADSS 20–23, which were recorded only for seven subjects. Error bars represent SD in CADSS subscores across subjects. *Subscales that were significantly different ($p_{uncorrected} < .05$) between baseline and during the ketamine scan. (With false discovery rate correction, all marked subscales had $p < .13$.)

all brain regions in Figure 3) (Figures 2–4). On average, there was a 21.3% decrease in regional V_T after ketamine challenge across all regions and subjects. The average ketamine-induced change in V_T (across all subjects) was 20% ± 23% in the anterior cingulate (Figure 4A), 20% ± 22% in the medial prefrontal cortex (Figure 4B), 20% ± 22% in the orbital prefrontal cortex, 20% ± 22% in the ventral striatum (Figure 4C), 21% ± 20% in the parietal lobe, 22% ± 21% in the dorsal putamen, 20% ± 22% in the dorsal caudate (Figure 4D), 25% ± 21% in the amygdala (Figure 4E), and 22% ± 20% in the hippocampus. Similar to the high binding regions, the cerebellum showed high variability in binding change (average binding decrease, 16.4% ± 18.8%; range: 42.4% decrease to 14.1% increase) (Figure 4F). The red lines in Figure 4 indicate the change in average regional V_T after ketamine administration.

Blood ketamine levels were variable, with averages (over the first 30 min) ranging from 82 ± 65 ng/mL to 202 ± 30 ng/mL. No significant correlations were observed between CADSS subscores (average, amnesia, depersonalization, or derealization) and ketamine levels. No significant correlations were observed between CADSS subscores or total injected amount of ketamine or ketamine concentration in blood and average V_T percent change.

Discussion

The goal of this study was to develop a paradigm to measure ketamine-induced changes in mGluR5 availability as an index of glutamate release using PET and [^{11}C]ABP688. We provide first evidence that ketamine administration decreases [^{11}C]ABP688 binding in vivo in human subjects. Increases in heart rate, blood pressure, and self-report on a questionnaire of dissociative symptoms were in line with ketamine effects.

We observed a global reduction of ~20% in [^{11}C]ABP688 binding with ketamine administration. It is conventional to compare such changes with changes measured in test/retest scans. Using a test/retest design, preclinical literature shows excellent reproducibility of [^{11}C]ABP688 binding (5%–10%) (33,43,61), although human studies are less consistent (32,34). Burger *et al.* (34) found high reproducibility between bolus and bolus/infusion studies in five healthy male volunteers scanned a few weeks apart (average percent difference <1%). However, we reported an increase (19.7%, on average) in [^{11}C]ABP688 binding during the second (same day afternoon) scan of a bolus test/retest paradigm (32). In the present study, the average binding decreased in the second (ketamine) scan. This effect is likely not attributable to tracer binding variability and could potentially be underestimated because of the test-retest effects we previously reported.

In this study, changes in V_T, which include both specific and nonspecific binding, were measured. It was not possible to measure specific binding directly because a region devoid of mGluR5 receptors in the human brain does not exist; there is no reference region to be used for this ligand (43,62,63). Without a true estimate of the nondisplaceable binding (V_{ND}), specific binding potential (BP_P or BP_{ND}) cannot be reliably estimated directly. We estimated BP_{ND} using a previously described technique (data not shown). Kågedal *et al.* (63) administered an mGluR5 negative allosteric modulator (AZD6200) to healthy human subjects and used a nonlinear mixed effects model to estimate

Table 2. Mean and Standard Deviation for Ratings Acquired Before, During, and After Ketamine Scan

	Baseline	During Ketamine Scan	60 Minutes After Ketamine Scan
CADSS (Amnesia, $n = 9$)	.0 ± .0	5.3 ± 3.9[a]	.2 ± .7
CADSS (Depersonalization, $n = 9$)	.1 ± .3	12.1 ± 7.1[a]	.8 ± 2.3
CADSS (Derealization, $n = 9$)	1.1 ± 1.6	.1 ± .3[a]	.9 ± 1.6
POMS T	.0 ± .0	.3 ± .7	.2 ± .6
POMS D	.6 ± 1.6	.7 ± 4.3	.5 ± 1.1
POMS A	1.6 ± 2.4	4.3 ± 4.5	3.3 ± 4.5
POMS F	3.2 ± 1.1	4.5 ± 5.2	3.9 ± 2.0
POMS C	4.4 ± 2.5	5.2 ± 7.7	5.1 ± 4.7
POMS V	2.2 ± 6.4	7.7 ± 1.5	4.2 ± 11.1
POMS Total	3.1 ± 4.4	1.5 ± .0	.9 ± 1.7
BDI	.0 ± .0		3 ± 3.5
HDRS	.6 ± 1.1		.9 ± 1.2
MADRS	.2 ± .6		.0 ± .0 ($n = 3$)

Statistics were calculated using all 10 subjects, unless otherwise indicated. Baseline ratings were performed before the first scan except in the case of the POMS, which was acquired before the ketamine scan. No significant differences were observed in POMS, BDI, HDRS, or MADRS scores at the different intervals.

A, anger-hostility; C, confusion-bewilderment; CADSS, Clinician Administered Dissociative State Scale; D, depression-dejection; F, fatigue-inertia; POMS, Profile of Mood States; BDI, Beck Depression Inventory; FDR, false discovery rate; HDRS, Hamilton Rating Scale for Depression; MADRS, Montgomery–Åsberg Depression Rating Scale; T, tension-anxiety; V, vigor-activity.

[a]Amnesia, $p = .035$, FDR = 12.5%; depersonalization, $p = .009$, FDR = 8.6%; derealization, $p = .004$, FDR = 8.6%.

mGluR5 occupancy and V_{ND} in the cerebellum simultaneously. By fixing the ratio of cerebellar nonspecific to specific binding to that estimated by Kågedal *et al.* (1.33), we estimated V_{ND} from baseline images and used it to estimate BP_{ND} (in the baseline and ketamine images). Using this estimate, as expected, percentage changes in [^{11}C]ABP688 BP_{ND} were slightly larger than the changes observed using V_T with evidence of a scan by region interaction (anterior cingulate 28% ± 30%, medial prefrontal cortex 29% ± 31%, orbital prefrontal cortex 29% ± 31%, ventral striatum 29% ± 30%, parietal lobe 30% ± 29%, dorsal putamen 32% ± 30%, dorsal caudate 30% ± 33%, amygdala 38% ± 30%, and hippocampus 34% ± 29%, all region-specific $p < .001$, based on the linear mixed effects model).

Results indicate that [^{11}C]ABP688 V_T decreased in all brain regions. Given that [^{11}C]ABP688 and glutamate bind at different sites on the receptor, this decrease should not be due to direct competition. However, the mechanism responsible for the change in [^{11}C]ABP688 binding is unclear. Previously, it was shown that *N*-acetyl-L-cysteine administration to baboons, which increases extrasynaptic glutamate levels through activating the cystine-glutamate antiporter, reduced [^{11}C]ABP688 binding (10%–20% of BP_{ND}) (33). The authors hypothesized that the decrease in BP_{ND} (proportional to the affinity of the radiotracer for the binding site) represented a reduction in tracer affinity in response to increase in glutamate. This mechanism requires further investigation because a similar investigation in rhesus monkeys did not replicate this effect (41). One potential mechanism is through increased mGluR5 internalization, which reduces ligand affinity by altering the local intracellular milieu. Regardless of the method by which mGluR5 affinity is decreased, the clinical implication is that this reduced affinity is required for the downstream effects of ketamine. This implication is analogous to our understanding of selective serotonin reuptake inhibitors, in which desensitization of the serotonin 1A receptor (5-hydroxytryptamine 1A, 5-HT_{1A}) is known to occur after long-term exposure to selective serotonin reuptake inhibitors. Although the mechanism is still unknown, preclinical studies suggest that 5-HT_{1A} internalization may be one process by which this occurs (64,65). Preclinical studies have also shown that receptors such as 5-HT_{2A} and the dopamine D_2 receptor can experience rapid internalization (66,67), as may be the case with mGluR5. Similar preclinical studies will be needed for full understanding of ketamine-induced effects at mGluR5.

The relationship between ketamine-induced effects and mGluR5 binding also needs to be evaluated further. Although ketamine-induced dissociative symptoms were observed in this study, they were not correlated with changes in [^{11}C]ABP688 binding. This finding is most likely due to the small sample size and the limited range of behavioral score change (owing to the fact that these were healthy volunteers). It is also possible that these correlations would be found only after some threshold of V_T

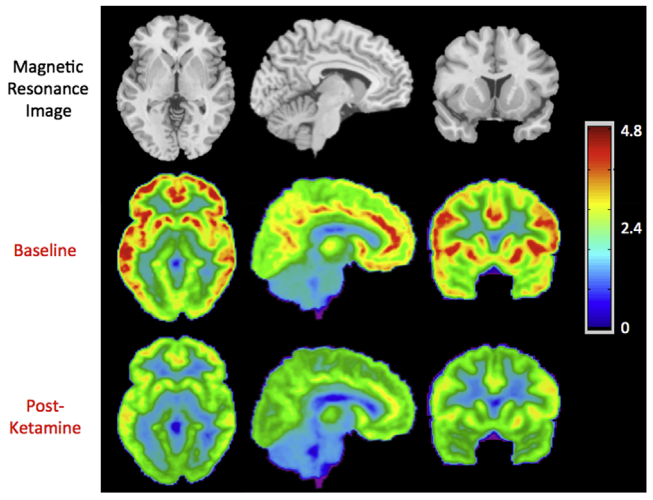

Figure 2. Average axial, sagittal, and coronal views of [^{11}C]ABP688 binding before and after ketamine administration. For each subject ($n = 10$), the volume of distribution (V_T) was calculated at every voxel. These images were warped into standard space using the Automatic Registration Toolbox (71), as previously described (55). The top row shows the magnetic resonance image template, for anatomic reference (72). The middle and bottom rows show the corresponding views of the mean [^{11}C]ABP688 V_T image. The V_T value associated with each color is indicated by the color bar.

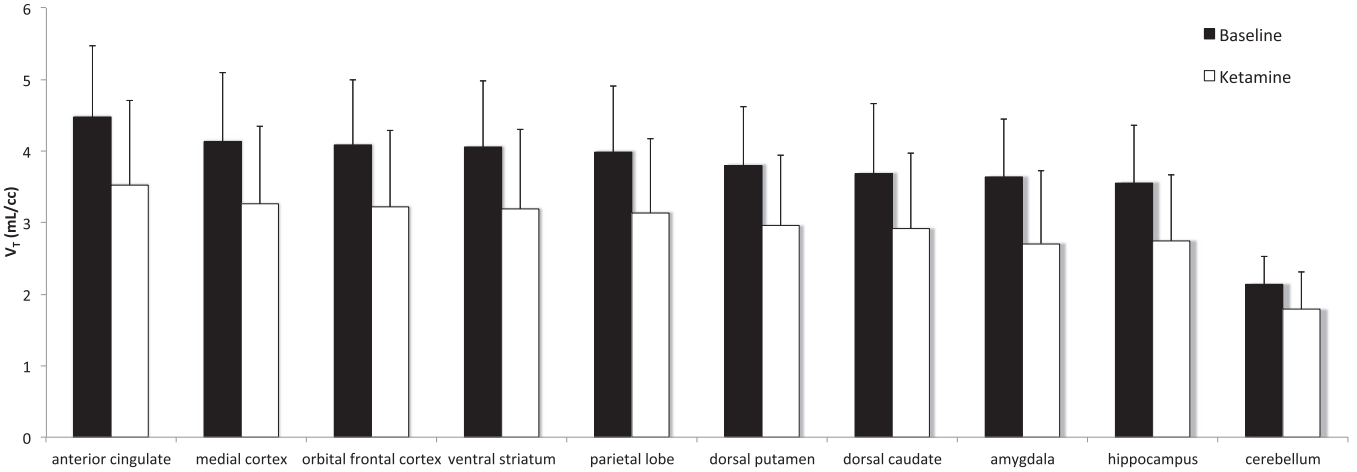

Figure 3. Average V_T across subjects ($n = 10$). Average values during the baseline scans (black bars) and challenge scans (white bars) are shown. Regions are organized from left to right in order of highest to lowest mean baseline binding. Differences in all regions shown are statistically significant ($p_{uncorrected} < .05$) in post hoc testing. Error bars represent SD across subjects. V_T, volume of distribution.

change is observed. In this study, seven subjects experienced <20% change in average V_T after ketamine infusion, and three subjects experienced >40% change; this makes uncovering correlations challenging. With a greater number of subjects, there will be more data available to examine correlations at higher percent differences.

As mentioned earlier, mGluR5 dysfunction has been implicated in models of disease, including depression and addiction. In this work, effects of ketamine treatment on mGluR5 were examined. However, to elucidate fully the pathways by which these ketamine-induced effects are clinically therapeutic, a greater understanding about both the role of mGluR5 in these diseases and the downstream effects of mGluR5 modulation are required. Imaging studies such as this would be useful for this purpose, shedding light on pathophysiology and potentially aiding in development of novel therapeutics.

This study has some limitations. The first limitation concerns the determination of mechanism. This study is the first to demonstrate an effect of ketamine administration on [^{11}C] ABP688 binding in humans. However, the mechanism by which this binding reduction occurs remains to be determined. For this reason, it is difficult to assess the cause of the intersubject variation in ketamine response. Although this variation may be due to individual differences in glutamate release after ketamine administration, as has been previously observed (20), further studies are needed to assess this possibility. Second, the study lacked a placebo group. All subjects were aware they were being administered ketamine and of ketamine's effects, and their subjective reports may have been influenced accordingly. However, because this study establishes the proof of concept, future studies can be conducted with a placebo group. With the paradigm established, future studies could be performed in a

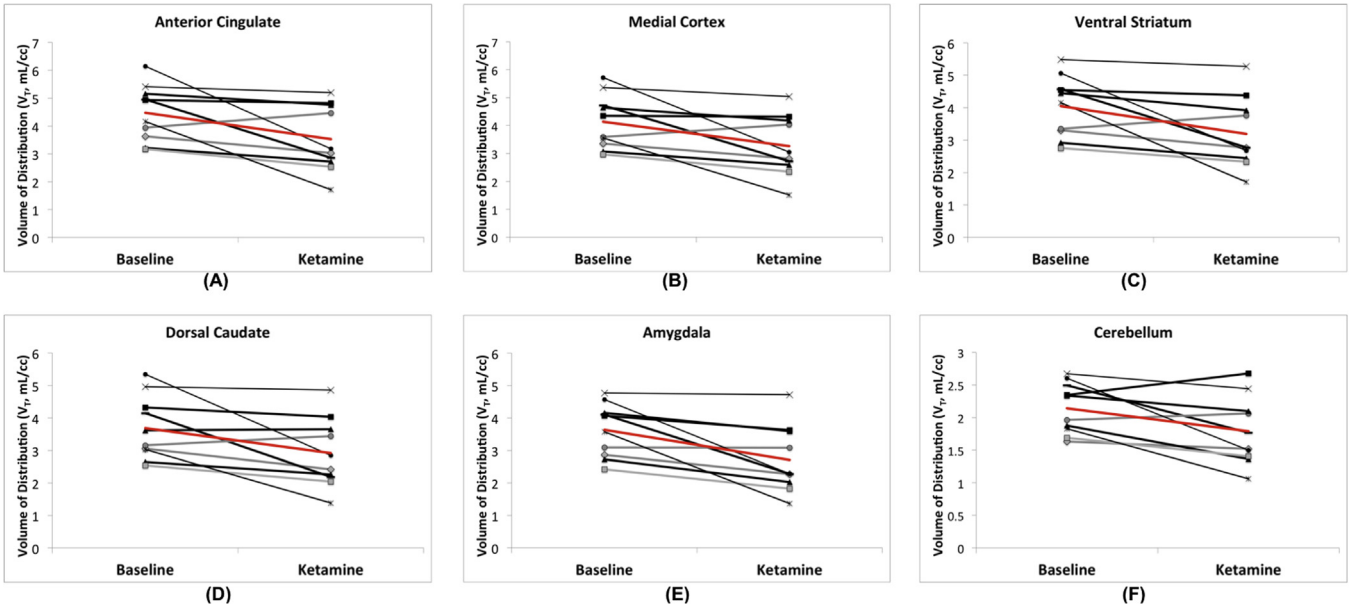

Figure 4. Effects of ketamine within each subject. The change in volume of distribution in high [anterior cingulate **(A)**, medial prefrontal cortex **(B)**, and ventral striatum **(C)**] and low [dorsal caudate **(D)**, amygdala **(E)**, and cerebellum **(F)**] binding regions is shown. Each line segment represents a different subject. Average change is indicated in red. V_T, volume of distribution.

depressed population, in which mGluR5 binding changes can be associated with response (to either ketamine or placebo). A third limitation concerns potential dynamic effects of ketamine that alter tracer delivery and washout. The kinetic modeling used assumes equilibrium conditions (59); however, blood pressure and heart rate were transiently elevated during ketamine administration. Ketamine has been shown to induce blood flow elevations in frontal regions (68–70), as measured with functional MRI, although the reported effect was not large and was localized to a few regions. A similar effect was observed in the present study, with region-dependent increases in tracer delivery (K_1) throughout the brain. Despite this effect, we did not detect significant changes in clearance between scans. Potential ketamine-induced changes (e.g., metabolism) are accounted for using the outcome measure V_T through the use of the metabolite-corrected arterial input function.

In conclusion, we developed a paradigm to measure ketamine-induced changes in [^{11}C]ABP688 binding in vivo in human subjects, which may reflect increases in endogenous glutamate. This finding raises the possibility that this pharmacologic-PET paradigm may be a useful approach for characterizing changes in regional brain glutamate release, a potentially important new strategy for studying the neurobiology and treatment of neuropsychiatric disorders.

This work was supported by National Institute of Mental Health (NIMH) Grant Nos. K01MH092681 (to IE) and K01MH091354 (to CD), Yale Center for Clinical Investigation Grant No. UL1RR024139 (to IE, JHK, REC, GS, MB), Nancy Taylor Foundation (to IE), U.S. Department of Veterans Affairs via its support of the National Center for Post Traumatic Stress Disorder (JHK, IE, GS), and National Institute on Alcohol Abuse and Alcoholism (NIAAA) Grant No. 2P50AA012879 (to JHK).

We thank the staff at the Yale University Positron Emission Tomography Center for their help with radiotracer syntheses and related analyses as well as imaging the subjects. We acknowledge the biostatistical consultation and support from the Biostatistical Consulting Core at the School of Medicine, Stony Brook University. We also thank Kiriana Morse for her diligent work in updating and editing the manuscript.

JJM receives royalties for commercial use of the Columbia-Suicide Severity Rating Scale from the Research Foundation for Mental Hygiene and has stock options in Qualitas Health, a start-up company working on a polyunsaturated fatty acid nutritional product. CA received a research fund or consultation fee from Genentech. JHK consults for several pharmaceutical and biotechnology companies, with compensation less than $10 000 per year, including AbbVie, Inc., Amgen, Astellas Pharma Global Development, AstraZeneca Pharmaceuticals, Biomedisyn Corporation, Bristol-Myers Squibb, Eli Lilly and Co., Janssen Research Development, Novartis, Sage Therapeutics, Inc., Sunovion Pharmaceuticals, Inc., Takeda Industries, Euthymics Bioscience, Inc., and Neurovance, Inc., a subsidiary of Euthymic Bioscience and Lundbeck Research USA. JHK is a member of the following scientific advisory boards: Lohocla Research Corporation, Mnemosyne Pharmaceuticals, Inc., Naurex, Inc., and Pfizer Pharmaceuticals. JHK is a past president of the American College of Neuropsychopharmacology, editor of Biological Psychiatry, and an employee of the Yale University School of Medicine and the U.S. Department of Veterans Affairs VA Connecticut Healthcare System. He is an originator on the following patent: J.P. Seibyl, J.H. Krystal, and D.S. Charney; Dopamine and Noradrenergic Reuptake Inhibitors in Treatment of Schizophrenia; Patent No. 5 447 948; 5 September 1995. JHK is an originator of the following relevant pending patents: Coric Vladimir, John H. Krystal, Gerard Sanacora; Glutamate Modulating Agents in the Treatment of Mental Disorders; US Patent No. 8,778,979, patent issue date: July 15, 2014; and D. Charney, J.H. Krystal, H. Manji, S. Matthew, C. Zarate; Intranasal Administration of Ketamine to Treat Depression; United States Application No. 14/197,767, filed on March 5, 2014. All other authors report no biomedical financial interests or potential conflicts of interest.

1. Cozzoli DK, Courson J, Caruana AL, Miller BW, Greentree DI, Thompson AB, *et al.* (2012): Nucleus accumbens mGluR5-associated signaling regulates binge alcohol drinking under drinking-in-the-dark procedures. *Alcohol Clin Exp Res* 36:1623–1633.
2. Spooren W, Ballard T, Gasparini F, Amalric M, Mutel V, Schreiber R (2003): Insight into the function of Group I and Group II metabotropic glutamate (mGlu) receptors: Behavioural characterization and implications for the treatment of CNS disorders. *Behav Pharmacol* 14: 257–277.
3. Akkus F, Ametamey SM, Treyer V, Burger C, Johayem A, Umbricht D, *et al.* (2013): Marked global reduction in mGluR5 receptor binding in smokers and ex-smokers determined by [11C]ABP688 positron emission tomography. *Proc Natl Acad Sci U S A* 110:737–742.
4. Deschwanden A, Karolewicz B, Feyissa A, Treyer V, Ametamey S, Johayem A, *et al.* (2011): Reduced metabotropic glutamate receptor 5 density in major depression determined by [11C]ABP688 PET and postmortem study. *Am J Psychiatry* 168:727–734.
5. Price R, Shungu D, Mao X, Nestadt P, Kelly C, Collins K, *et al.* (2009): Amino acid neurotransmitters assessed by proton magnetic resonance spectroscopy: Relationship to treatment resistance in major depressive disorder. *Biol Psychiatry* 65:792–800.
6. Yüksel C, Öngür D (2010): Magnetic resonance spectroscopy studies of glutamate-related abnormalities in mood disorders. *Biol Psychiatry* 68: 785–794.
7. Gigante A, Bond D, Lafer B, Lam R, Young L, Yatham L (2012): Brain glutamate levels measured by magnetic resonance spectroscopy in patients with bipolar disorder: A meta-analysis. *Bipolar Disord* 14: 478–487.
8. Paul IA, Skolnick P (2003): Glutamate and depression: Clinical and preclinical studies. *Ann N Y Acad Sci* 1003:250–272.
9. aan het Rot M, Collins KA, Murrough JW, Perez AM, Reich DL, Charney DS, Mathew SJ (2010): Safety and efficacy of repeated-dose intravenous ketamine for treatment-resistant depression. *Biol Psychiatry* 67: 139–145.
10. aan Het Rot M, Zarate CA Jr, Charney DS, Mathew SJ (2012): Ketamine for depression: Where do we go from here? *Biol Psychiatry* 72:537–547.
11. Murrough JW, Perez AM, Pillemer S, Stern J, Parides MK, aan het Rot M, *et al.* (2013): Rapid and longer-term antidepressant effects of repeated ketamine infusions in treatment-resistant major depression. *Biol Psychiatry* 74:250–256.
12. Niciu MJ, Luckenbaugh DA, Ionescu DF, Mathews DC, Richards EM, Zarate CA Jr (2013): Subanesthetic dose ketamine does not induce an affective switch in three independent samples of treatment-resistant major depression. *Biol Psychiatry* 74:e23–24.
13. Murrough JW, Wan LB, Iacoviello B, Collins KA, Solon C, Glicksberg B, *et al.* (2013): Neurocognitive effects of ketamine in treatment-resistant major depression: Association with antidepressant response [published online ahead of print Sep 11]. *Psychopharmacology (Berl).*
14. Murrough JW, Iosifescu DV, Chang LC, Al Jurdi RK, Green CE, Perez AM, *et al.* (2013): Antidepressant efficacy of ketamine in treatment-resistant major depression: A two-site randomized controlled trial. *Am J Psychiatry* 170:1134–1142.
15. Berman RM, Cappiello A, Anand A, Oren DA, Heninger GR, Charney DS, Krystal JH (2000): Antidepressant effects of ketamine in depressed patients. *Biol Psychiatry* 47:351–354.
16. Zarate CA Jr, Singh JB, Carlson PJ, Brutsche NE, Ameli R, Luckenbaugh DA, *et al.* (2006): A randomized trial of an N-methyl-D-aspartate antagonist in treatment-resistant major depression. *Arch Gen Psychiatry* 63:856–864.
17. Lorrain D, Baccei C, Bristow L, Anderson J, Varney M (2003): Effects of ketamine and N-methyl-D-aspartate on glutamate and dopamine

release in the rat prefrontal cortex: Modulation by a group II selective metabotropic glutamate receptor agonist LY379268. *Neuroscience* 117: 697–706.
18. Moghaddam B, Adams B, Verma A, Daly D (1997): Activation of glutamatergic neurotransmission by ketamine: A novel step in the pathway from NMDA receptor blockade to dopaminergic and cognitive disruptions associated with the prefrontal cortex. *J Neurosci* 17: 2921–2927.
19. Chowdhury GM, Behar KL, Cho W, Thomas MA, Rothman DL, Sanacora G (2012): (1)H-[(1)(3)C]-nuclear magnetic resonance spectroscopy measures of ketamine's effect on amino acid neurotransmitter metabolism. *Biol Psychiatry* 71:1022–1025.
20. Stone JM, Dietrich C, Edden R, Mehta MA, De Simoni S, Reed LJ, *et al.* (2012): Ketamine effects on brain GABA and glutamate levels with 1H-MRS: Relationship to ketamine-induced psychopathology. *Mol Psychiatry* 17:664–665.
21. Li N, Lee B, Liu RJ, Banasr M, Dwyer JM, Iwata M, *et al.* (2010): mTOR-dependent synapse formation underlies the rapid antidepressant effects of NMDA antagonists. *Science (New York, NY)* 329:959–964.
22. Li N, Liu R, Dwyer J, Banasr M, Lee B, Son H, *et al.* (2011): Glutamate N-methyl-D-aspartate receptor antagonists rapidly reverse behavioral and synaptic deficits caused by chronic stress exposure. *Biol Psychiatry* 69:754–761.
23. Niesters M, Khalili-Mahani N, Martini C, Aarts L, van Gerven J, van Buchem M, *et al.* (2012): Effect of subanesthetic ketamine on intrinsic functional brain connectivity: A placebo-controlled functional magnetic resonance imaging study in healthy male volunteers. *Anesthesiology* 117:868–877.
24. Scheidegger M, Walter M, Lehmann M, Metzger C, Grimm S, Boeker H, *et al.* (2012): Ketamine decreases resting state functional network connectivity in healthy subjects: Implications for antidepressant drug action. *PloS One* 7:e44799.
25. Esterlis I, Hannestad J, Bois F, Sewell R, Tyndale R, Seibyl J, *et al.* (2013): Imaging changes in synaptic acetylcholine availability in living human subjects. *J Nucl Med* 54:78–82.
26. Frankle W, Cho R, Narendran R, Mason N, Vora S, Litschge M, *et al.* (2009): Tiagabine increases [11C]flumazenil binding in cortical brain regions in healthy control subjects. *Neuropsychopharmacology* 34: 624–633.
27. Thompson JL, Urban N, Slifstein M, Xu X, Kegeles L, Girgis R, *et al.* (2013): Striatal dopamine release in schizophrenia comorbid with substance dependence. *Mol Psychiatry* 18:909–915.
28. Narendran R, Jedema H, Lopresti B, Mason N, Gurnsey K, Ruszkiewicz J, *et al.* (2014): Imaging dopamine transmission in the frontal cortex: A simultaneous microdialysis and [(11)C]FLB 457 PET study. *Mol Psychiatry* 19:302–310.
29. Guo N, Guo W, Kralikova M, Jiang M, Schieren I, Narendran R, *et al.* (2010): Impact of D2 receptor internalization on binding affinity of neuroimaging radiotracers. *Neuropsychopharmacology* 35:806–817.
30. Sullivan J, Lim K, Labaree D, Lin S, McCarthy T, Seibyl J, *et al.* (2013): Kinetic analysis of the metabotropic glutamate subtype 5 tracer [(18)F] FPEB in bolus and bolus-plus-constant-infusion studies in humans. *J Cereb Blood Flow Metab* 33:532–541.
31. Wong D, Waterhouse R, Kuwabara H, Kim J, Brašić J, Chamroonrat W, *et al.* (2013): 18F-FPEB, a PET radiopharmaceutical for quantifying metabotropic glutamate 5 receptors: A first-in-human study of radiochemical safety, biokinetics, and radiation dosimetry. *J Nucl Med* 54: 388–396.
32. DeLorenzo C, Kumar JD, Mann J, Parsey R (2011): In vivo variation in metabotropic glutamate receptor subtype 5 binding using positron emission tomography and [^{11}C]ABP688. *J Cereb Blood Flow Metab* 31: 2169–2180.
33. Miyake N, Skinbjerg M, Easwaramoorthy B, Kumar D, Girgis R, Xu X, *et al.* (2011): Imaging changes in glutamate transmission in vivo with the metabotropic glutamate receptor 5 tracer [11C] ABP688 and N-acetylcysteine challenge. *Biol Psychiatry* 69:822–824.
34. Burger C, Deschwanden A, Ametamey S, Johayem A, Mancosu B, Wyss M, *et al.* (2010): Evaluation of a bolus/infusion protocol for 11C-ABP688, a PET tracer for mGluR5. *Nucl Med Biol* 37:845–851.
35. Brown AK, Kimura Y, Zoghbi SS, Siméon FG, Liow JS, Kreisl WC, *et al.* (2008): Metabotropic glutamate subtype 5 receptors are quantified in the human brain with a novel radioligand for PET. *Jm Nucl Med* 49: 2042–2048. doi:10.2967/jnumed.108.056291.
36. Hamilton M (1960): A rating scale for depression. *J Neurol Neurosurg Psychiatry* 23:56–62.
37. Montgomery SA, Asberg M (1979): A new depression scale designed to be sensitive to change. *Br J Psychiatry* 134:382–389.
38. Beck S, Ward C, Mendelsohn M, Erbaugh J (1961): An inventory for measuring depression. *Arch Gen Psychiatry* 4:561–571.
39. Bremner J, Krystal J, Putnam F, Southwick S, Marmar C, Charney D, Mazure C (1999): Measurement of dissociative states with the Clinician-Administered Dissociative States Scale (CADSS). *J Trauma Stress* 11:125–136.
40. Norcross J, Guadagnoli E, Prochaska J (1984): Factor structure of the profile of mood states (POMs), two partial replications. *J Clin Psychol* 40:1270–1277.
41. Sandiego CM, Nabulsi N, Lin SF, Labaree D, Najafzadeh S, Huang Y, *et al.* (2013): Studies of the metabotropic glutamate receptor 5 radioligand [(1)(1)C]ABP688 with N-acetylcysteine challenge in rhesus monkeys. *Synapse* 67:489–501.
42. Kawamura K, Yamasaki T, Kumata K, Furutsuka K, Takei M, Wakizaka H, *et al.* (2014): Binding potential of (E)-[(11)C]ABP688 to metabotropic glutamate receptor subtype 5 is decreased by the inclusion of its (11) C-labelled Z-isomer. *Nucl Med Biol* 41:17–23.
43. DeLorenzo C, Milak MS, Brennan KG, Kumar JS, Mann JJ, Parsey RV (2011): In vivo positron emission tomography imaging with [(11)C]ABP688: Binding variability and specificity for the metabotropic glutamate receptor subtype 5 in baboons. *Eur J Nucl Med Mol Imaging* 38:1083–1094.
44. Treyer V, Streffer J, Wyss MT, Bettio A, Ametamey SM, Fischer U, *et al.* (2007): Evaluation of the metabotropic glutamate receptor subtype 5 using PET and 11C-ABP688: Assessment of methods. *J Nucl Med* 48: 1207–1215.
45. Carson RE, Barker WC, Liow J-S, Johnson CA (2003): Design of a motion-compensation OSEM list-mode algorithm for resolution-recovery reconstruction for the HRRT. *Nuclear Science Symposium Conference Record, 2003 IEEE* 5:3281–3285.
46. Anticevic A, Gancsos M, Murray J, Repovs G, Driesen N, Ennis D, *et al.* (2012): NMDA receptor function in large-scale anti-correlated neural systems with implications for cognition and schizophrenia. *Proc Natl Acad Sci U S A* 109:16720–16725.
47. Driesen NR, McCarthy G, Bhagwagar Z, Bloch M, Calhoun V, D'Souza DC, *et al.* (2013): Relationship of resting brain hyperconnectivity and schizophrenia-like symptoms produced by the NMDA receptor antagonist ketamine in humans. *Mol Psychiatry* 18:1199–1204.
48. Krystal JH, Karper LP, Seibyl JP, Freeman GK, Delaney R, Bremner JD, *et al.* (1994): Subanesthetic effects of the noncompetitive NMDA antagonist, ketamine, in humans. Psychotomimetic, perceptual, cognitive, and neuroendocrine responses. *Arch Gen Psychiatry* 51:199–214.
49. Newcomer JW, Farber NB, Jevtovic-Todorovic V, Selke G, Melson AK, Hershey T, *et al.* (1999): Ketamine-induced NMDA receptor hypofunction as a model of memory impairment and psychosis. *Neuropsychopharmacology* 20:106–118.
50. Oye I, Paulsen O, Maurset A (1992): Effects of ketamine on sensory perception: Evidence for a role of N-methyl-D-aspartate receptors. *J Pharmacol Exp Ther* 260:1209–1213.
51. Neumeister A, Normandin MD, Murrough JW, Henry S, Bailey CR, Luckenbaugh DA, *et al.* (2012): Positron emission tomography shows elevated cannabinoid CB (1) receptor binding in men with alcohol dependence. *Alcohol Clin Exp Res* 36:2104–2109.
52. Rusjan PM, Wilson AA, Bloomfield PM, Vitcu I, Meyer JH, Houle S, Mizrahi R (2011): Quantitation of translocator protein binding in human brain with the novel radioligand [18F]-FEPPA and positron emission tomography. *J Cereb Blood Flow Metab* 31:1807–1816.
53. Gallezot JD, Nabulsi N, Neumeister A, Planeta-Wilson B, Williams WA, Singhal T, *et al.* (2010): Kinetic modeling of the serotonin 5-HT(1B) receptor radioligand [(11)C]P943 in humans. *J Cereb Blood Flow Metab* 30:196–210.
54. Wu S, Ogden RT, Mann JJ, Parsey RV (2007): Optimal metabolite curve fitting for kinetic modeling of 11C-WAY-100635. *J Nucl Med* 48:926–931.
55. DeLorenzo C, Kumar JS, Mann JJ, Parsey RV (2011): In vivo variation in metabotropic glutamate receptor subtype 5 binding using positron emission tomography and [11C]ABP688. *J Cereb Blood Flow Metab* 31: 2169–2180.
56. DeLorenzo C, Klein A, Mikhno A, Gray N, Zanderigo F, Mann JJ, Parsey RV (2009): *A new method for assessing PET-MRI coregistration*. In: *SPIE Medical Imaging*. Bellingham, WA: SPIE, 72592W–72598.

57. Logan J, Fowler JS, Volkow ND, Wolf AP, Dewey SL, Schlyer DJ, *et al.* (1990): Graphical analysis of reversible radioligand binding from time-activity measurements applied to [N-11C-methyl]-(-)-cocaine PET studies in human subjects. *J Cereb Blood Flow Metab* 10:740–747.
58. Patel S, Hamill T, Connolly B, Jagoda E, Li W, Gibson R (2007): Species differences in mGluR5 binding sites in mammalian central nervous system determined using in vitro binding with [18F]F-PEB. *Nucl Med Biol* 34:1009–1017.
59. Innis RB, Cunningham VJ, Delforge J, Fujita M, Gjedde A, Gunn RN, *et al.* (2007): Consensus nomenclature for in vivo imaging of reversibly binding radioligands. *J Cereb Blood Flow Metab* 27:1533–1539.
60. Hirvonen J, Johansson J, Teras M, Oikonen V, Lumme V, Virsu P, *et al.* (2008): Measurement of striatal and extrastriatal dopamine transporter binding with high-resolution PET and [11C]PE2I: Quantitative modeling and test-retest reproducibility. *J Cereb Blood Flow Metab* 28: 1059–1069.
61. Elmenhorst D, Aliaga A, Bauer A, Rosa-Neto P (2012): Test-retest stability of cerebral mGluR(5) quantification using [(1)(1)C]ABP688 and positron emission tomography in rats. *Synapse* 66:552–560.
62. Patel S, Hamill TG, Connolly B, Jagoda E, Li W, Gibson RE (2007): Species differences in mGluR5 binding sites in mammalian central nervous system determined using in vitro binding with [18F]F-PEB. *Nucl Med Biol* 34:1009–1017.
63. Kågedal M, Cselényi Z, Nyberg S, Raboisson P, Ståhle L, Stenkrona P, *et al.* (2013): A positron emission tomography study in healthy volunteers to estimate mGluR5 receptor occupancy of AZD2066—estimating occupancy in the absence of a reference region. *Neuroimage* 82:160–169.
64. Bouaziz E, Emerit MB, Vodjdani G, Gautheron V, Hamon M, Darmon M, Masson J (2014): Neuronal phenotype dependency of agonist-induced internalization of the 5-HT(1A) serotonin receptor. *J Neurosci* 34: 282–294.
65. Riad M, Rbah L, Verdurand M, Aznavour N, Zimmer L, Descarries L (2008): Unchanged density of 5-HT(1A) autoreceptors on the plasma membrane of nucleus raphe dorsalis neurons in rats chronically treated with fluoxetine. *Neuroscience* 151:692–700.
66. Berry SA, Shah MC, Khan N, Roth BL (1996): Rapid agonist-induced internalization of the 5-hydroxytryptamine2A receptor occurs via the endosome pathway in vitro. *Mol Pharmacol* 50:306–313.
67. Macey TA, Gurevich VV, Neve KA (2004): Preferential Interaction between the dopamine D2 receptor and Arrestin2 in neostriatal neurons. *Mol Pharmacol* 66:1635–1642.
68. Breier A, Malhotra A, Pinals D, Weisenfeld N, Pickar D (1997): Association of ketamine-induced psychosis with focal activation of the prefrontal cortex in healthy volunteers. *Am J Psychiatry* 154:805–811.
69. Vollenweider F, Leenders K, Scharfetter C, Antonini A, Maguire P, Missimer J, Angst J (1997): Metabolic hyperfrontality and psychopathology in the ketamine model of psychosis using positron emission tomography (PET) and [18F]fluorodeoxyglucose (FDG). *Eur Neuropsychopharmacol* 7:9–24.
70. Rowland L, Beason-Held L, Tamminga C, Holcomb H (2010): The interactive effects of ketamine and nicotine on human cerebral blood flow. *Psychopharmacology* 208:575–584.
71. Ardekani BA, Guckemus S, Bachman A, Hoptman MJ, Wojtaszek M, Nierenberg J (2005): Quantitative comparison of algorithms for inter-subject registration of 3D volumetric brain MRI scans. *J Neurosci Methods* 142:67–76.
72. Holmes CJ, Hoge R, Collins L, Woods R, Toga AW, Evans AC (1998): Enhancement of MR images using registration for signal averaging. *J Comput Assist Tomogr* 22:324–333.